Precambrian Research 231 (2013) 194–205

Contents lists available at SciVerse ScienceDirect

Precambrian Research

journal homepage: www.elsevier.com/locate/precamres

U–Pb systematics in carbonates of the Postmasburg Group, Transvaal Supergroup, South Africa: Primary *versus* metasomatic controls

Brenton Fairey[a], Harilaos Tsikos[a], Fernando Corfu[b,*], Stéphane Polteau[c]

[a] Geology Department, Rhodes University, PO Box 94, Grahamstown 6140, South Africa
[b] Department of Geosciences, University of Oslo, PO Box 1047, Blindern, Oslo 0316, Norway
[c] Volcanic Basin Petroleum Research AS, Forskningsparken, Gaustadalléen 21, 0349 Oslo, Norway

ARTICLE INFO

Article history:
Received 29 August 2012
Received in revised form 6 March 2013
Accepted 18 March 2013
Available online 2 April 2013

Keywords:
Postmasburg Group
Mooidraai Formation
Makganyene Formation
Carbonates
U–Pb geochronology
Metasomatism

ABSTRACT

Petrography, geochemistry and U–Pb geochronology of a section through the Mooidraai carbonates which overly the Hotazel iron formation in the Postmasburg Group of the Transvaal Supergroup, and comparison with previous work, demonstrate different degrees of localized metasomatic overprints causing chemical changes and affecting the U–Pb isotopic features of the rocks. The lower parts of the section in drillhole OLP-2, at the transition from iron formation to carbonates, exhibit extensive formation of riebeckite in concordant seams and layers, probably crystallized in response to addition of Na from early pore water or brines. Mooidraai limestone samples throughout the section are characterized by the extensive development of stylolites, which are enriched in U with respect to intervening massive carbonate laminae. The latter preserve Pb–Pb systematics close to those documented previously in dolomitized Mooidraai Formation, whereas the stylolites have strongly discordant U–Pb systems. The U–Pb data define an upper intercept age of 2392 ± 23 Ma, which confirms the previous Pb–Pb age of the formation, and a lower intercept age of 588 ± 31 Ma, which is interpreted to reflect a metasomatic overprint, also recorded elsewhere in the wider region by Ar–Ar dating of hydrothermal minerals. The combined available geochronological record indicates the occurrence of several extensive episodes of fluid-controlled metasomatism, apparently representing the far-field response to distal orogenic processes. The initial Pb composition of the Mooidraai carbonates is much less radiogenic than that in carbonates associated with the stratigraphically lower Makganyene diamictite Formation, reflecting a provenance of the Pb from erosion of older Archean crust rather than a typical sea-water signal as recorded in the Mooidraai carbonates.

1. Introduction

The Palaeoproterozoic was a remarkable period in the evolution of the Earth, being characterized by prolonged tectonic quiescence and continental stability interspersed by severe paleoclimatic crises, and with fundamental changes in the composition of the atmosphere accompanying the transition from anoxic to oxygenated conditions and the related biological consequences (*e.g.* Holland and Beukes, 1990; Bekker et al., 2004; Hannah et al., 2004; Melezhik, 2006; Guo et al., 2009; Tsikos et al., 2010). The study of these events has been done mainly using the record stored in the extensive platformal sedimentary sequences covering all the Archean cratons. Among these sequences, the Transvaal Supergroup, which covers the Kaapvaal craton in South Africa, has played a central role due to its good stratigraphic preservation, the variety of depositional settings and conditions, and not least the economic importance of the region (Moore et al., 2001, 2012; Tsikos et al., 2003).

The correct reading and understanding of the Transvaal stratigraphic record, however, has been hampered by a number of problems. The main difficulties concern the separation of primary depositional effects from secondary overprints of metasomatic nature, a challenge affecting mainly the proper analysis and interpretation of the isotopic record. This is a particular problem for the Postmasburg Group in the Northern Cape Province, where there remain fundamental disagreements on the age of deposition of some of the successions and on the significance of some of the isotopic and mineralogical records (Moore et al., 2001, 2011; Tsikos et al., 2010). In this study we have addressed some of these questions, focusing mainly on the Mooidraai Formation, a shallow marine carbonate sequence overlying banded iron-formation (BIF) and manganese ore of the Hotazel Formation in the uppermost part of the Transvaal Supergroup (Tsikos et al., 2001; Bau and Alexander, 2006). Previous work has shown that different parts of the sequence are mineralogically distinct, raising the question of properly separating primary depositional features from

* Corresponding author. Tel.: +47 22 85 66 80; fax: +47 22 85 42 15.
E-mail address: fernando.corfu@geo.uio.no (F. Corfu).

0301-9268/$ – see front matter © 2013 Elsevier B.V. All rights reserved.
http://dx.doi.org/10.1016/j.precamres.2013.03.010

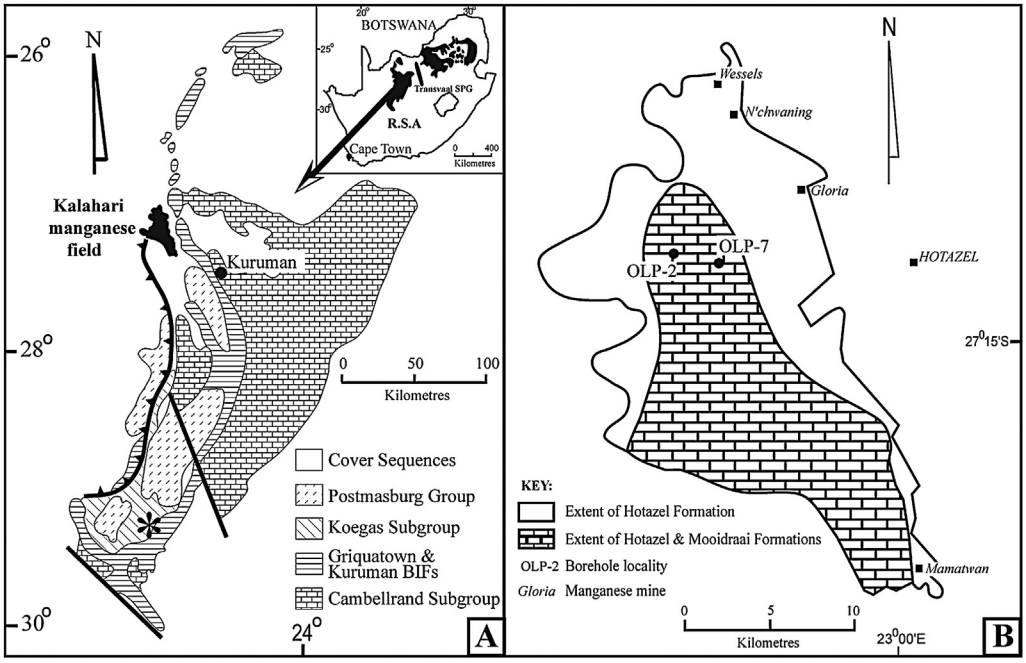

Fig. 1. (A) Simplified geological map of the Transvaal Supergroup and location of the Kalahari Manganese Field in the Northern Cape Province, South Africa. The star indicates the field locality of the Makganyene Formation bioherms sampled for this study. (B) Localities of drillcores OLP-2 (this study) and OLP-7 (Tsikos et al., 2001) in the Kalahari Manganese Field.

those of superimposed metasomatic effects. This paper assesses the petrography, textural relationships and geochemistry across the transition from the Hotazel to the Mooidraai Formation, and places special emphasis on compaction and dissolution-related structures (stylolites).

A particular problem affecting this sequence is the age of deposition, expressed by a fundamental conflict between a whole-rock Pb–Pb age of 2222 ± 12 Ma obtained for the underlying volcanic Ongeluk Formation (Walraven et al., 1990; Cornell et al., 1996) and a Pb–Pb age of 2394 ± 26 Ma reported for the younger carbonates of the Mooidraai Formation (Bau et al., 1999). This discrepancy has far-reaching consequences for the regional correlation of the Transvaal stratigraphy (Moore et al., 2001, 2012) and also for global correlation of isotopic anomalies (Bau et al., 1999). In this study we have therefore undertaken a new set of experiments using the U–Pb system and obtained results that confirm the older (~2.4 Ga) age of deposition of the carbonates. Additionally, we provide new insights into superimposed metasomatic processes involving gain of U, and uncover more evidence on an enigmatic Ediacaran event which has evidently affected these sequences. Finally, we also tested the Pb composition of carbonates within the glacial Makganyene Formation which lies at the base of the Postmasburg Group, obtaining a crude isochron age consistent with the existing age framework but with a very distinct initial ratio, indicating a much stronger contribution from old cratonic material in the diamictite than in the later platformal sediments.

2. Geological background

The Transvaal Supergroup is a platformal sedimentary succession composed of three distinct unconformity-bound sequences exposed in two main areas, namely the Transvaal Basin in the east and the Griqualand West basin at the western margin of the Kaapvaal craton, and extending northward into Botswana (Moore et al., 2001, 2012). This paper is focused on the Postmasburg Group, which is the stratigraphically uppermost sequence in the Griqualand West basin (Figs. 1 and 2).

The base of the Postmasburg Group is represented by the Makganyene Formation, which consists of glacial diamictite with locally intercalated calcareous bioherms in its lower part, ranging laterally into sandstones and shales (Polteau et al., 2006). This unit is overlain by the Ongeluk Formation of basaltic andesite and hyaloclastic breccias (Beukes, 1983), with pillow basalts indicating submarine deposition. The overlying Hotazel Formation is the youngest BIF member in the Transvaal succession, and hosts important manganese deposits in the form of three discrete sedimentary layers. The Hotazel Formation and its contained Mn ores are developed in an area known as the Kalahari Manganese Field (Fig. 1). The BIF itself is typically microbanded, with magnetite-rich bands

Supergroup	Group	Subgroup	Formation	Lithology
Olifantshoek			Mapedi	Shale, quartzite and conglomerate
Transvaal Supergroup (Griqualand West)	Postmasburg	Voelwater	Mooidraai	Carbonate and minor chert
			Hotazel	Iron-formation and Mn ore
			Ongeluk	Andesitic lavas
			Makganyene	Glacial diamictite
	Ghaap	Koegas		Siliciclastics and iron-formation
		Asbestos Hills	Griquatown	Clastic-textured iron-formation
			Kuruman	Microbanded iron-formation
		Campbellrand		Carbonate and minor shale
		Schmidtsdrif		Shale, quartzite, carbonate and lava

Fig. 2. Stratigraphy of the Transvaal Supergroup showing the regional angular unconformity between the Transvaal and Olifantshoek Supergroups.
Modified after Tsikos et al. (2001).

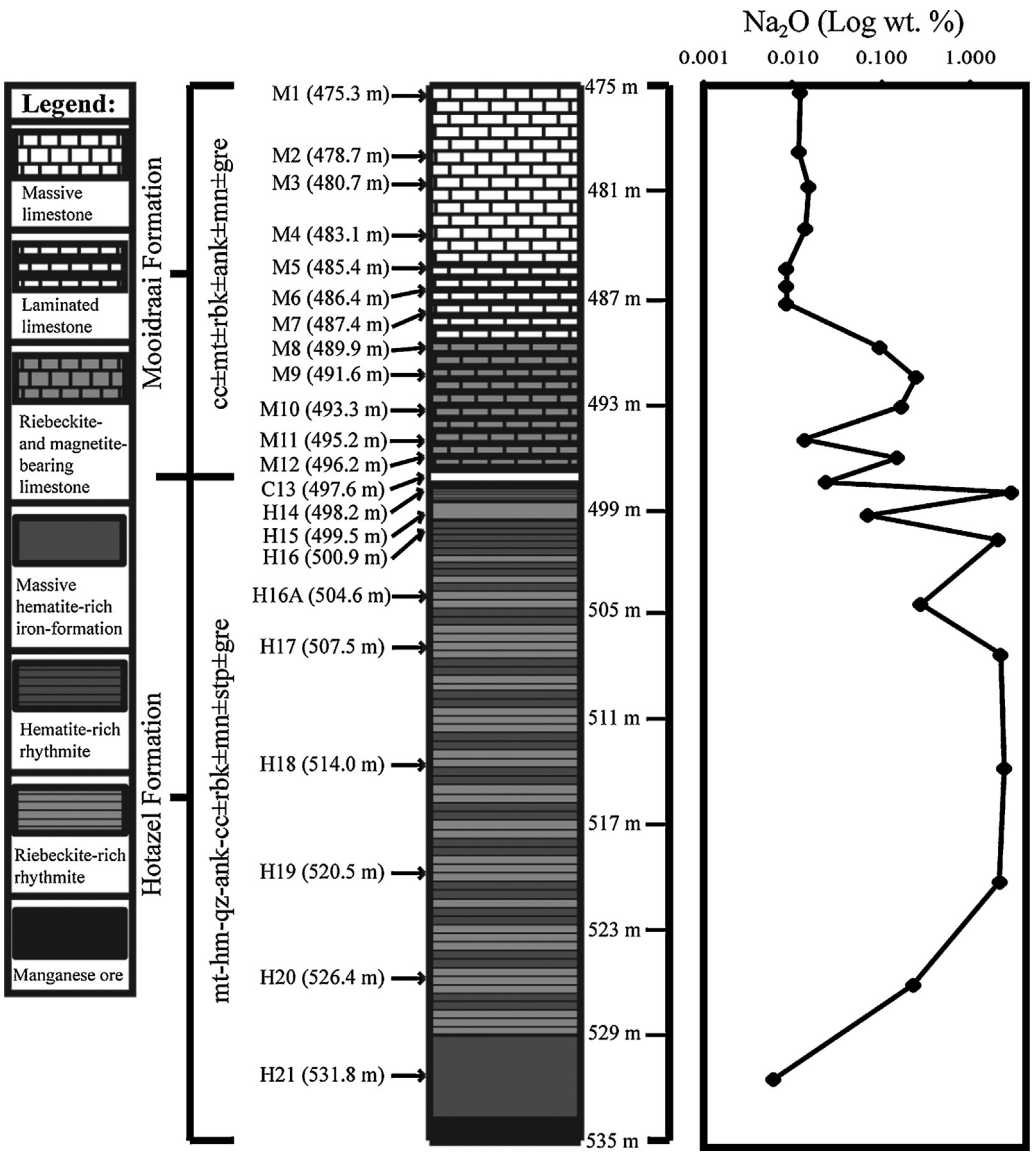

Fig. 3. Detailed log of diamond drill core OLP-2. *Note*: mt = magnetite; hm = hematite; qz = quartz; ank = ankerite; cc = calcite; rbk = riebeckite; mn = minnesotaite; sd = siderite; stp = stilpnomelane; gre = greenalite.

alternating with chert-rich ones containing a variety of Fe–silicate and Fe–carbonate minerals. The Hotazel BIF records a broad increase in modal carbonate stratigraphically upwards, and ultimately grades into the carbonate-dominated Mooidraai Formation (Tsikos et al., 2001). Although Beukes (1983) and Bau et al. (1999) describe the Mooidraai Formation as predominantly chert-bearing dolomite, later work by Tsikos et al. (2001) and this study show that dolomitisation was a local phenomenon not persistent throughout the Kalahari Manganese Field. The Mooidraai Formation in the study area is approximately 90 m thick and consists of undolomitised and unsilicified Fe-bearing laminated limestone, similar to the one studied by Tsikos et al. (2001).

Over most part of the Kalahari Manganese Field, the Mapedi Formation of the Olifantshoek Supergroup lies unconformably either above the Mooidraai Formation, or directly atop the Hotazel BIF-Mn Formation. This unconformity has a regional character, as the basal Mapedi shales are seen elsewhere in the wider region to unconformably overly the stratigraphically lower BIFs (mainly the Kuruman BIF) and associated hematitic iron-ores of the Ghaap Group (Fig. 2). This unconformity has also been previously implicated as a potential structural conduit for hydrothermal fluid flow and resultant Fe/Mn ore-formation (Beukes et al., 2003; Tsikos et al., 2003). Locally, however, the Mooidraai Formation is directly overlain by the unconformable Paleozoic Dwyka Group of the Karoo Supergroup, and this is also the case in the drillcore intersection OLP-2 examined in this study.

The age of the Postmasburg Group has been problematic and controversial (Moore et al., 2001, 2012). Metavolcanic rocks of the Ongeluk Formation were studied by Walraven et al. (1990), who reported a whole-rock Pb–Pb age, subsequently refined to 2222 ± 12 Ma by Cornell et al. (1996). This age conflicted, however, with a whole-rock Pb–Pb isochron age of 2394 ± 26 Ma determined by Bau et al. (1999) for stratigraphically younger, highly silicified Mooidraai dolomite. Although not entirely decisive, U–Pb ages for detrital zircon in samples of the Makganyene and Hotazel Formations support the older ~2.4 Ga age of the Postmasburg Group (Moore et al., 2012).

3. Materials and methods

A total of 23 half-core samples were collected from diamond drillcore OLP-2, which samples the upper part of the Hotazel

Formation as well as the lower stratigraphic portion of the Mooidraai Formation. The borehole is located on the farm Olivepan in the Kalahari Manganese Field (Fig. 1). Mineral compositions were investigated with transmitted light microscopy, X-ray diffraction (XRD), and Scanning Electron Microscopy-Energy Dispersive Spectroscopy (SEM-EDS). Bulk-rock major and trace element concentrations for 22 of the 23 samples were determined by X-ray fluorescence (XRF), according to the method of Norrish and Hutton (1969). In addition, the major element composition of carbonates in the Makganyene Formation bioherms was analyzed with an electron microprobe. All these analyses were performed using in-house analytical facilities at Rhodes University Moore et al. (2011).

Whole-rock powders for ten samples of the Makganyene Formation bioherms were reacted with pure phosphoric acid at 50 °C, using the evolved CO_2 to analyze the isotopic composition of C and O at the University of Cape Town (Tsikos et al., 2001).

Small parts of drillcore OLP-2, and three Mooidraai powder samples from core OLP-7 previously studied by Tsikos et al. (2001), were used for the U–Pb isotopic study of carbonates of the Mooidraai Formation. In addition, some tests were also done on rock fragments of dolomitic bioherms of the Makganyene Formation (Polteau et al., 2006). For the U–Pb isotopes, the solid samples were washed with water on a hot-plate and rinsed with acetone. These, and the powders, were then weighed, spiked with a ^{202}Pb–^{205}Pb–^{235}U tracer, and transferred to a Savillex vial for dissolution with HCl on a hot plate. The solution was purified with anion exchange resin, some through a single-stage HBr–HCl separation and others through a two-stage HBr and HCl–HNO_3 separation. Measurements were carried out on a MAT 262 mass spectrometer. Other details are given in Corfu (2004). The decay constants are from Jaffey et al. (1971). Plotting and calculation were done using the program Isoplot (Ludwig, 2003).

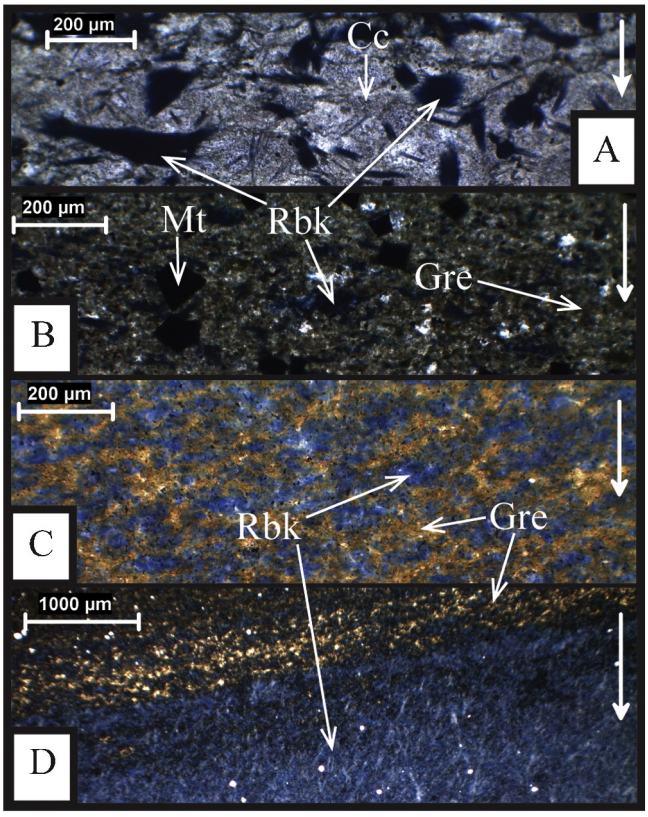

Fig. 4. Riebeckite-rich laminae and textures across the upper Hotazel BIF and lower Mooidraai Formation, drillcore OLP-2. All images were taken using plane-polarized light. Top-down vertical white arrows indicate arrangement of images according to stratigraphic depth. (A) Riebeckite-bearing band. (B) Single band rich in greenalite and riebeckite. (C) Riebeckite disseminations in a magnetite-bearing greenalite-chert band with minor ankerite. (D) Riebeckite "sprays" set in Mooidraai limestone.

4. Petrography of the Hotazel and Mooidraai Formations

Fig. 3 gives a detailed log of the transition between the Hotazel Formation and the Mooidraai Formation. Samples H21 to H14 represent *ca.* 32 m of BIF from the upper portion of the Hotazel Formation. Sample C13 is from the contact between the Hotazel and Mooidraai Formations, whilst M12 to M1 sample the bottom ~21 m of the Mooidraai Formation.

The mineralogy of the Hotazel BIF sampled here compares well with results from earlier studies (Tsikos and Moore, 1997; Tsikos et al., 2003). Common minerals are quartz, magnetite, ankerite, calcite, riebeckite, stilpnomelane, greenalite, minnesotaite, and minor hematite. Magnetite is the most abundant iron-bearing mineral. It occurs as 50 up to 250 μm euhedral grains, either in massive, mm-thick laminae or disseminated in chert-rich bands. Hematite was found only at the contact with the overlying Mooidraai carbonates (sample C13) and in sample H21 taken from a unit known as hematite lutite, which generally forms the hanging- and footwall of the manganese ore bodies (Tsikos et al., 2003). In both samples, the hematite is extremely fine-grained and appears dull-red to brown, both in hand-specimen and under the microscope.

Quartz occurs as microcrystalline aggregates (chert) dominating the matrix of Fe-poor bands. Iron–silicate species include minnesotaite, greenalite, stilpnomelane and riebeckite. Minnesotaite occurs locally as disseminated, less than 50 μm needles or sprays and with highly variable modal abundance on a band-to-band scale. Stilpnomelane is locally developed as disseminated, fine-grained laths, particularly in proximity to magnetite laminae along with calcite, and around magnetite grain boundaries. Greenalite is present in very fine-grained form in chert bands along with variable modal amounts of interspersed riebeckite, minnesotaite and lesser carbonate. Ankerite is the most dominant carbonate, present in disseminations or massive laminae with lesser calcite, quartz and Fe silicate minerals. Its characteristic rhombohedral shape is very well preserved in many of the disseminated grains. Calcite is the second most dominant carbonate, associated with ankerite in carbonate-rich bands and stilpnomelane near the contacts with magnetite-rich laminae.

Riebeckite is locally very abundant in the samples of this study, contrary to the previously studied domains of the Hotazel BIF (Tsikos and Moore, 1997; Tsikos et al., 2003). It generally forms disseminations within chert and lesser Fe–silicate minerals (mainly greenalite), but also essentially massive, mono-mineralic laminae, ~100 μm to ~1 cm thick (Fig. 4B–D). The contact of the Hotazel BIF with the Mooidraai Formation is defined by a succession of riebeckite-rich BIF overlain by a chert layer containing very fine-grained hematite and lesser stilpnomelane. The basal ~2 cm of the overlying Mooidraai Formation is characterized by a ~2 cm-thick intraclastic calcareous layer that reflects syn-sedimentary slumping. Above the latter, the Mooidraai Formation consists predominantly of massive, microcrystalline calcite together with minor ankerite. Riebeckite disseminations are seen only in the bottom *ca.* 8 m of the drillcore section (Figs. 3 and 4A). Minor, disseminated silicates (quartz, greenalite and minnesotaite) as well as magnetite also occur locally across the entire sampled section. Texturally, the Mooidraai Formation, particularly in its lower part, exhibits visible micro-laminations to mm-scale banding defined by modal variations in the abundance of Fe-bearing minerals relative to carbonate.

Evidence of dissolution and re-precipitation is pervasive throughout the entire sampled portion of the Mooidraai Formation.

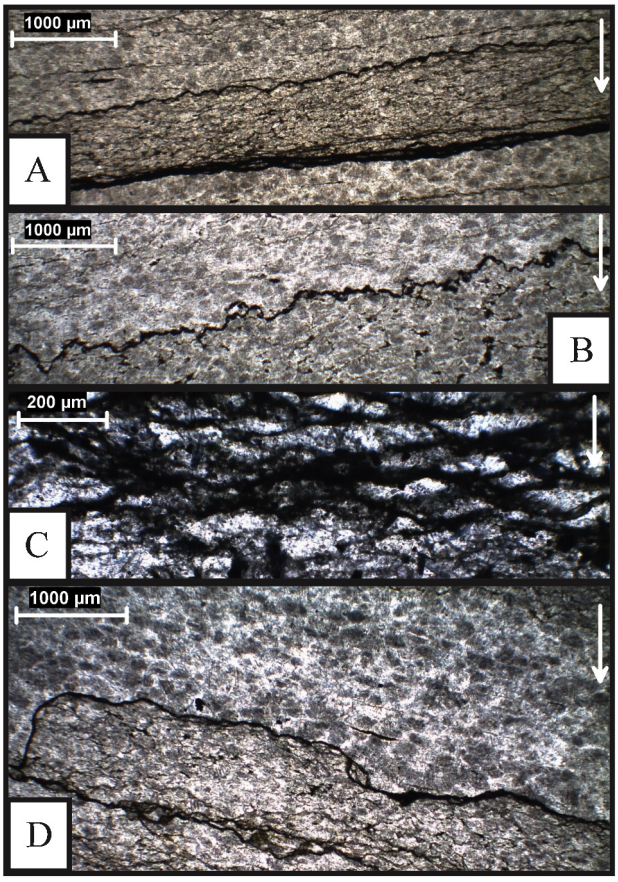

Fig. 5. Stylolite textures in the Mooidraai Formation, drillcore OLP-2. All images were taken using plane-polarized light. Top-down vertical white arrows indicate arrangement of images according to stratigraphic depth. (A) Thick stylolites show smoother profiles than thinner ones. Dark lenses above the upper stylolite are incipient dissolution surfaces, common throughout the sequence. (B) Thin stylolite showing well-defined jagged interlocking projections. (C) Anastomosing stylolites, common in most samples examined in this study; in some cases, a number of such stylolites coalesce into larger (~0.5 cm) ones. (D) Two stylolites have coincidentally merged, increasing the thickness of the resultant dissolution interface.

This is typically expressed by the development of stylolites parallel or sub-parallel to the lamination and sedimentary layering (Fig. 5A–D). The stylolites consist of submicroscopic material. Back-scattered electrons and SEM-EDS identify Fe–oxide (probably magnetite) toward the center and greenalite lining the dissolution surfaces of the stylolites (Fig. 6).

5. Geochemical results

5.1. Bulk geochemistry of the Hotazel and Mooidraai Formations

The samples of the Mooidraai Formation in drillcore OLP-2 consist predominantly of CaO (ranging from 39 to 48 wt%) with <1 wt% MgO and 1–8 wt% SiO_2 (Table 1). The second most abundant oxide is Fe_2O_3 (3–14 wt%). By contrast, SiO_2 and Fe_2O_3 dominate the Hotazel Formation, with lesser CaO (0.5–8 wt% CaO) and 1–3 wt% MgO. As expected, the abundance of Na_2O correlates very well with the amount of riebeckite: parts with massive riebeckite bands contain up to 2 wt% Na_2O or more, whereas parts with disseminated riebeckite have generally less than 0.5 wt% Na_2O (Fig. 3).

Similarly to previously published results (Tsikos et al., 2001) the most abundant trace element in the Mooidraai Formation is Sr (1300–2200 ppm), substituting for Ca in calcite. All other trace elements are either below detection of the XRF technique or at levels generally not exceeding 15 ppm. The Hotazel Formation also has Sr as the main trace element (40–440 ppm) associated with calcite, and contains 20–200 ppm Ba. Transition metals such as Zn, Cu, Cr and V are present in concentrations generally below 30 ppm, whilst all other trace elements measured are either below 12 ppm or undetectable.

5.2. U–Pb isotopic systematics of the Mooidraai Formation

Halved sections of samples M1 and M4 from drillcore OLP-2 were used for the isotopic work (Fig. 3). The selected specimens represent massive micro-laminated limestone, heterogeneous on a mm-scale, with alternations of homogeneous gray to white carbonate, green-streaked, greenalite-bearing carbonate and carbonate with thin black coated stylolites. The initial selection was aimed at exploring possible variations in U–Pb and radiogenic Pb abundances between different parts of the rock. Subsequent analyses

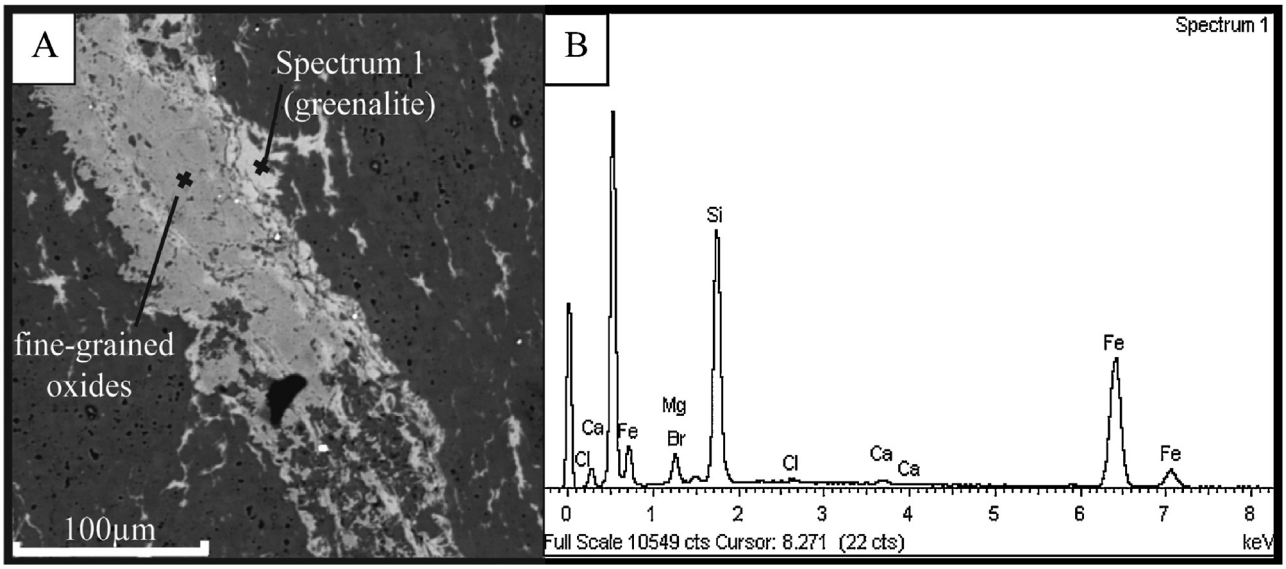

Fig. 6. SEM-EDS backscatter image (A) and qualitative mineral analyses (B) of stylolitic material from the Mooidraai Formation show the presence of greenalite on the edges with fine-grained oxides (possibly magnetite) in the center.

Table 1
Major and trace element analyses of the Mooidraai and Hotazel Formations.

Sample number	Mooidraai Formation												Hotazel Formation								
	M1	M2	M3	M4	M5	M6	M7	M8	M9	M10	M11	M12	H14	H15	H16	H16A	H17	H18	H19	H20	H21
Depth (m) wt%	475.3	478.7	480.7	483.1	485.4	486.4	487.4	489.9	491.6	493.3	495.2	496.2	498.2	499.5	500.9	504.6	507.5	514	520.5	526.4	531.8
SiO_2	2.58	1.66	1.61	2.20	3.48	4.11	4.27	6.39	7.84	6.01	6.49	5.86	51.16	33.86	35.64	37.61	36.89	42.21	39.26	32.72	24.90
TiO_2	0.04	0.04	0.03	0.03	0.03	0.03	0.03	0.04	0.03	0.03	0.03	0.04	0.01	0.05	0.03	0.03	0.03	0.03	0.03	0.03	0.05
Al_2O_3	0.45	0.07	0.05	0.06	0.06	0.06	0.06	0.07	0.07	0.05	0.06	0.09	0.02	0.41	0.03	0.07	0.01	b.d	b.d	b.d	b.d
Fe_2O_3	3.63	3.61	3.34	4.38	6.90	8.51	8.77	11.92	13.50	10.98	12.27	10.89	35.55	40.60	56.08	44.83	40.85	45.14	42.45	52.83	53.15
MnO	0.73	0.68	0.72	0.69	0.52	0.67	0.69	0.68	0.68	0.75	0.67	0.56	0.05	0.20	0.05	0.38	0.13	0.07	0.08	0.12	1.53
MgO	1.00	0.90	0.88	0.93	1.11	1.10	1.08	1.13	1.22	1.19	1.30	1.33	3.09	3.12	2.07	2.32	2.09	2.50	1.96	1.43	1.33
CaO	48.50	46.14	47.03	46.44	45.12	43.28	42.87	41.89	39.07	40.96	39.87	41.12	0.61	4.36	0.85	4.89	7.02	1.58	5.87	5.34	7.63
Na_2O	0.01	0.01	0.01	0.01	0.01	0.01	0.01	0.10	0.25	0.17	0.01	0.15	2.94	0.07	2.08	0.28	2.23	2.45	2.19	0.23	0.01
K_2O	0.35	0.32	0.33	0.32	0.31	0.30	0.31	0.30	0.28	0.29	0.29	0.30	0.10	0.18	0.09	0.07	0.11	0.07	0.09	0.07	0.10
P_2O_5	0.13	0.12	0.12	0.12	0.12	0.12	0.12	0.12	0.12	0.12	0.12	0.12	0.08	0.08	0.08	0.05	0.06	0.06	0.13	0.13	0.09
LOI	41.60	43.93	45.30	43.88	41.21	40.77	40.71	37.03	36.42	38.37	37.84	38.69	5.48	15.87	1.74	8.34	9.95	4.10	6.57	6.48	10.24
H_2O^-	0.87	1.55	0.28	0.25	0.30	0.32	0.37	0.37	0.43	0.32	0.35	0.29	0.46	0.66	0.52	0.40	0.72	0.42	0.42	0.26	0.36
Total (ppm)	99.88	99.03	99.71	99.33	99.17	99.29	99.27	100.04	99.89	99.22	99.30	99.45	99.54	99.47	99.26	99.28	100.08	98.63	99.05	99.63	99.38
Zr	b.d	b.d	b.d	b.d	3	2	2	1	b.d	b.d	b.d	2	3	11	2	5	3	4	4	5	4
Y	3	2	3	3	3	3	3	3	5	4	3	5	10	13	8	8	7	10	11	11	10
Sr	1433	1188	1387	1356	1204	1377	1477	1958	1852	1804	1444	1367	41	207	59	279	435	80	294	190	274
Rb	b.d	b.d	b.d	b.d	b.d	b.d	b.d	b.d	b.d	b.d	b.d	b.d	3	13	2	3	3	3	1	1	5
Zn	8	8	8	11	10	14	12	16	14	14	8	13	29	19	39	22	16	23	30	14	18
Cu	8	8	9	10	9	10	12	13	13	13	10	11	14	17	19	19	17	17	19	21	23
Ba	n.d	n.d	n.d	n.d	n.d	n.d	n.d	n.d	n.d	n.d	n.d	n.d	25	211	37	22	97	52	71	30	82
Sc	n.d	n.d	n.d	n.d	n.d	n.d	n.d	n.d	n.d	n.d	n.d	n.d	1	5	1	3	2	2	2	3	2
Co	b.d	b.d	b.d	b.d	4	5	4	b.d	b.d	4	b.d	b.d	2	4	3	5	3	4	4	5	12
Cr	2	b.d	b.d	b.d	2	2	2	b.d	3	2	2	2	9	16	13	14	11	13	13	25	23
V	b.d	b.d	b.d	b.d	b.d	b.d	4	5	4	b.d	b.d	4	7	16	6	8	5	8	7	11	12
Ce	11	15	13	19	11	14	12	11	7	10	16	8	6	11	3	5	6	0	4	3	3
Nd	13	18	16	18	13	11	13	11	8	12	16	10	2	6	1	3	3	2	3	0	2

Note: n.d.: not determined; b.d.: below detection limit; ppm: parts per million; wt%: weight percent.

were focused mainly on stylolite coatings, as well as on clean carbonate, in order to obtain more information on the discordance of the analyses. In addition, powders from three samples from drillcore OLP-7 analyzed by Tsikos et al. (2001) were also used. The samples in this section contain higher non-carbonate components than samples M1 and M4 from drillcore OLP-2, although they have only rare stylolites.

Twelve analyses were obtained from fragments of sample M1 and five analyses from M4. They yielded between 0.1 and 0.6 ppm Pb and 0.08 to 1.52 ppm U, the U content increasing greatly in the fragments with black stylolite coatings (Table 2). The $^{206}Pb/^{204}Pb$ ratios vary from 26 to 64, mostly in consonance with the U content. When plotted on a Pb–Pb diagram (Fig. 7A) the data are not collinear but follow instead an arcuate array. A regression line has a slope corresponding to about 2100 Ma, but with a large scatter. The three analyses obtained from sample powders of drillcore OLP-7 are less radiogenic that those from OLP-2, and plot on or close to the Pb–Pb regression line reported by Bau et al. (1999). As an example, a calculation using the eight least radiogenic values of Bau et al. (1999) and two OLP-7 analyses, yields an MSWD of 1.0 and an age of 2403 ± 26 Ma (Fig. 7B). The line also passes through the two least radiogenic analyses of sample M1 from drillcore OLP-2 (Fig. 7B), a common twelve point regression defining an age of 2422 ± 20 Ma, with an MSWD of 1.6 (not shown). The remaining analyses plot below these regression lines, the deviation increasing with increasing $^{206}Pb/^{204}Pb$ ratios.

The reason for the deviation becomes evident when the corresponding U–Pb data are examined in a Concordia diagram (Fig. 8). Essentially all of the data are discordant, three reversely and the rest normally discordant. The U–Pb data all have rather low $^{206}Pb/^{204}Pb$ ratios, and are thus very sensitive to the common Pb correction used. Because of the disturbed U–Pb systematics and the related discordance of the data, it is not possible to extrapolate back to the initial Pb by removing the radiogenic component from each analysis. The Pb–Pb isotopic systematics (Fig. 7B), however, strongly suggest that the initial Pb composition for these rocks must be located on the Pb–Pb isochron, and its most likely position is at the intersection of the isochron with paleo-isochrons drawn from 2400 Ma to 3400, 3200 and 3000 Ma, the main age range of rocks from the underlying Kaapvaal craton. The starting points of the paleo-isochrons were calculated with the Stacey and Kramers (1975) model, which approximates average crustal compositions. The box shown in Fig. 7B covers the range of these intersections and corresponds to $^{206}Pb/^{204}Pb = 15.0$ (±1%) and $^{207}Pb/^{204}Pb = 15.3$ (±0.5%). The value is considered a reasonable estimate for the initial Pb composition in the Mooidraai carbonates.

The U–Pb analyses corrected using this extrapolated composition follow a common general trend but are not collinear: all 17 analyses define a line with an MSWD of 6.3. Four of the analyses deviate to the left of the main array. Regression of the other 13 analyses yields a discordia line with an upper intercept age of 2392 ± 23 Ma and a lower intercept age of 588 ± 31 Ma.

5.3. Geochemistry and U–Pb systematics of the Makganyene Formation bioherms

The Makganyene Formation bioherms are essentially massive siliceous dolostones, composed of >80% modal Fe-bearing dolomite (FeO: 3.0 ± 2.6 wt%; MnO: 0.7 ± 0.5 wt%; MgO: 18.9 ± 2.3 wt%), set in a very fine-grained matrix of microcrystalline quartz and lesser calcite. Bulk-rock $\delta^{13}C$ and $\delta^{18}O$ values range between −4.9 and −1.5‰ (*vs.* VPDB) and 16–27‰ (*vs.* SMOW), respectively. In a δ–δ diagram (Fig. 9), the isotope results define a broadly linear relationship which compares well with that seen in samples of the Mooidraai Formation (Tsikos et al., 2001). We interpret the latter relationship, the ferroan nature of dolomite and the relatively low $\delta^{13}C$ values of bulk carbonate in the bioherms, as collectively indicative of isotopic fractionation processes in the diagenetic environment involving organic carbon mineralization. These are likely to have involved the reduction of primary ferric iron species and concomitant oxidation of the organic carbon *via* microbial dissimilatory iron reduction. The latter process is variously considered to have dominated biogeochemical redox cycling in Palaeoproterozoic anoxic basins (Johnson et al., 2008; Heimann et al., 2010; Craddock and Dauphas, 2011).

The four U–Pb analyses performed on these samples are unradiogenic due to very low U contents of 0.036–0.054 ppm and initial common Pb contents of 0.33–0.66 ppm. Hence no meaningful U–Pb data can be considered in this case. The Pb–Pb data (Table 2 and Fig. 7B) nevertheless show some degree of isotopic variation and define an isochron with a good fit (MSWD = 0.66), corresponding to an age of 2441 ± 200 Ma. Although the uncertainty is very large, the nominal age is meaningful as it fits well into the general age framework (Bau et al., 1999; Moore et al., 2012). An interesting aspect of these data is their distinctly higher initial Pb ratio than for the Mooidraai carbonates, indicating a provenance of Pb from more evolved crustal sources. This may reflect strong glacial erosion of U-rich and/or older granitic crust at this time, against a sea-water composition controlled by less evolved material during deposition of the Mooidraai carbonate sediments.

6. Discussion

6.1. Geochemical and mineralogical variations between sample suites

There is a striking variation in the mineralogy and composition of the limestone suites at different sites of the Mooidraai Formation. The samples analyzed by Bau et al. (1999) are strongly silicified and dolomitized, with SiO_2 contents of 40–47 wt% *versus* 1–8 wt% in our samples and MgO of 10–12 wt% *versus* ~1 wt% or less, respectively (OLP-2 and -7; Table 1, and Tsikos et al., 2001). Another remarkable difference is the very low abundance of Sr in the samples of Bau et al. (1999; 13–15 ppm) *versus* 1000–2000 ppm in our studied suite, and an opposite trend in the REE abundance with 0.22–0.27 ppm Ce in the Bau et al. (1999) samples, up to 10 times lower than in the OLP-7 samples of (0.4–2.6 ppm; Tsikos et al., 2001), and 30–80 times lower than in the OLP-2 series studied here (Table 1). Another set of striking contrasts is the concentration of U, which is around 0.04–0.05 ppm in Bau et al. (1999) series but between two and thirty times larger in drillcore OLP-2 (0.08–1.5 ppm; Table 2) and with only one value of 0.24 ppm available for OLP-7 (Table 2), whereas the content of Pb goes the other way from values of 2.1–2.7 ppm in the Bau et al. (1999) samples to 0.1–0.6 ppm in OLP-2 and intermediate values in OLP-7 (Table 2). All these contrasting characteristics are likely to reflect variable overprint by different processes at different times and different locations.

Dolomitization of limestones is generally linked to replacement processes by Mg-enriched brines during diagenesis (*e.g.* Merino and Canals, 2011, and references therein). Silicification of the Mooidraai dolomite post-dates the dolomitization, as indicated by deposition of silica in vugs and veins and corrosion of carbonate grains, and was associated with the deposition of pyrite (Bau et al., 1999). These replacement processes reduced the amount of Ca present, explaining the different Ca concentration in dolomite and limestone. It is not clear whether the removal of Ca also explains the absence of Sr, since the abundance of the latter is reduced much more greatly than that of the Ca.

The abundance of riebeckite above and below the contact between the Hotazel and Mooidraai Formations, as illustrated in Figs. 3 and 4, is a feature that has hitherto not been addressed

Table 2
U–Pb and Pb–Pb data for Mooidraai and Makganyene carbonates.

Properties[a]	Weight (μg)	U (ppm)	Pbt (ppm)[b]	Pbi (ppm)[c]	206/204[d]	2σ (%)	207/204[d]	2σ (%)	208/204[d]	2σ (%)	207/235[e]	2σ (abs)[e]	206/238[e]	2σ (abs)[e]	rho[f]	207/206[e]	2σ (abs)[e]	206/238 (Ma)	2σ (abs)
Mooidraai Formation – drillhole OLP-2; Core 25; 475.55 m; Box 51																			
gr, 2 bl-l	374	0.18	0.44	0.32	32.067	0.44	17.730	0.35	37.37	0.40	10.92	0.42	0.5561	0.0055	0.20	0.1424	0.0054	2851	23
g-l	987	0.09	0.26	0.20	26.827	0.22	17.171	0.23	36.64	0.30	10.63	0.48	0.4874	0.0065	0.10	0.1582	0.0073	2560	28
w	479	0.08	0.20	0.15	29.401	0.58	17.532	0.39	37.42	0.50	10.43	0.46	0.4881	0.0076	0.31	0.1550	0.0065	2562	33
gr	2276	0.08	0.13	0.09	34.159	0.31	18.180	0.28	37.91	0.40	8.35	0.26	0.4030	0.0034	0.15	0.1503	0.0046	2183	16
g, bl-l	1577	0.13	0.18	0.12	36.393	0.35	18.253	0.31	38.34	0.40	6.65	0.20	0.3495	0.0027	0.18	0.1380	0.0042	1932	13
w, g-l	864	0.11	0.14	0.09	38.943	0.66	18.836	0.36	38.37	0.50	7.01	0.26	0.3442	0.0099	0.74	0.1477	0.0037	1907	47
gr, m bl-l	2827	0.13	0.14	0.08	43.876	0.43	19.646	0.47	40.28	0.60	6.84	0.17	0.3357	0.0034	0.41	0.1479	0.0034	1866	16
gr, bl-c	270	0.36	0.29	0.18	44.77	1.3	19.198	0.75	39.06	0.90	4.82	0.16	0.2669	0.0019	0.43	0.1309	0.0040	1525	10
w, bl-c	433	0.46	0.23	0.11	64.21	1.3	21.606	0.59	41.53	0.70	3.92	0.07	0.2216	0.0028	0.66	0.1282	0.0018	1290	15
gr, m-bl-l, bl-c	190	0.57	0.32	0.18	51.65	1.8	19.827	0.71	39.57	0.80	3.60	0.08	0.2115	0.0012	0.30	0.1235	0.0027	1237	6
w, 1 bl-c	182	0.66	0.30	0.16	58.75	2.2	20.575	0.87	39.72	1.00	3.17	0.06	0.1910	0.0010	0.28	0.1206	0.0022	1127	5
gr, bl-c	11	1.52	0.61	0.34	55.14	21	19.71	6.6	40.00	8.00	2.46	0.12	0.1624	0.0035	0.46	0.1098	0.0049	970	19
Mooidraai Formation – drillhole OLP-2; Core 1; 484.15 m; Box 52																			
w	19,295	0.11	0.16	0.10	39.039	0.32	18.909	0.42	38.90	0.40	8.31	0.24	0.4014	0.0031	0.32	0.1502	0.0042	2175	14
gr, bl-c	655	0.33	0.47	0.34	31.447	0.24	17.491	0.23	39.64	0.30	5.56	0.22	0.3026	0.0029	0.11	0.1332	0.0052	1704	15
ge, bl-c	3494	0.30	0.23	0.13	51.845	0.19	20.461	0.20	42.54	0.30	5.52	0.09	0.2856	0.0014	0.17	0.1401	0.0023	1620	7
gr, bl-l, bl-c	852	0.31	0.21	0.11	58.976	0.73	21.056	0.39	43.57	0.40	5.01	0.08	0.2778	0.0016	0.27	0.1309	0.0021	1580	8
w, bl-c	451	0.30	0.25	0.15	44.243	0.82	19.324	0.41	41.81	0.40	5.15	0.12	0.2712	0.0017	0.22	0.1376	0.0031	1547	8
Mooidraai Formation – drillhole OLP-7																			
Powder #2	1860	0.24	0.70	0.58	22.637	0.14	16.378	0.19	37.70	0.30									
Powder #5	1490	–	1.97	1.77	18.295	0.13	15.767	0.19	36.50	0.30									
Powder #6	1660	–	0.45	0.39	21.091	0.04	16.225	0.19	35.66	0.30									
Makganyene Formation bioherms, MK08																			
gr #1	2166	0.036	0.38	0.33	19.183	0.15	16.255	0.20	36.08	0.30									
gr #5	4477	0.054	0.71	0.65	17.744	0.13	16.019	0.19	35.71	0.30									
gr (g) #5	2133	0.044	0.71	0.65	17.604	0.14	15.991	0.20	35.63	0.30									
gr #3	33,443	–	–	–	18.983	0.15	16.202	0.18	36.35	0.30									

[a] Limestone fragments: gr = gray; g = light green; bl-l = black layers; bl-c = black-coating; g-l = green layers; w = white.
[b] Pbt = total amount of Pb.
[c] Pbi = initial amount of Pb.
[d] Common Pb compositions, corrected for fractionation and blank.
[e] Data corrected for fractionation, blank and initial common Pb, the latter using a composition of 206/204 = 15.0 (±1%) and 207/204 = 15.3 (±0.5%) (see Fig. 7B).
[f] rho = correlation coefficient.

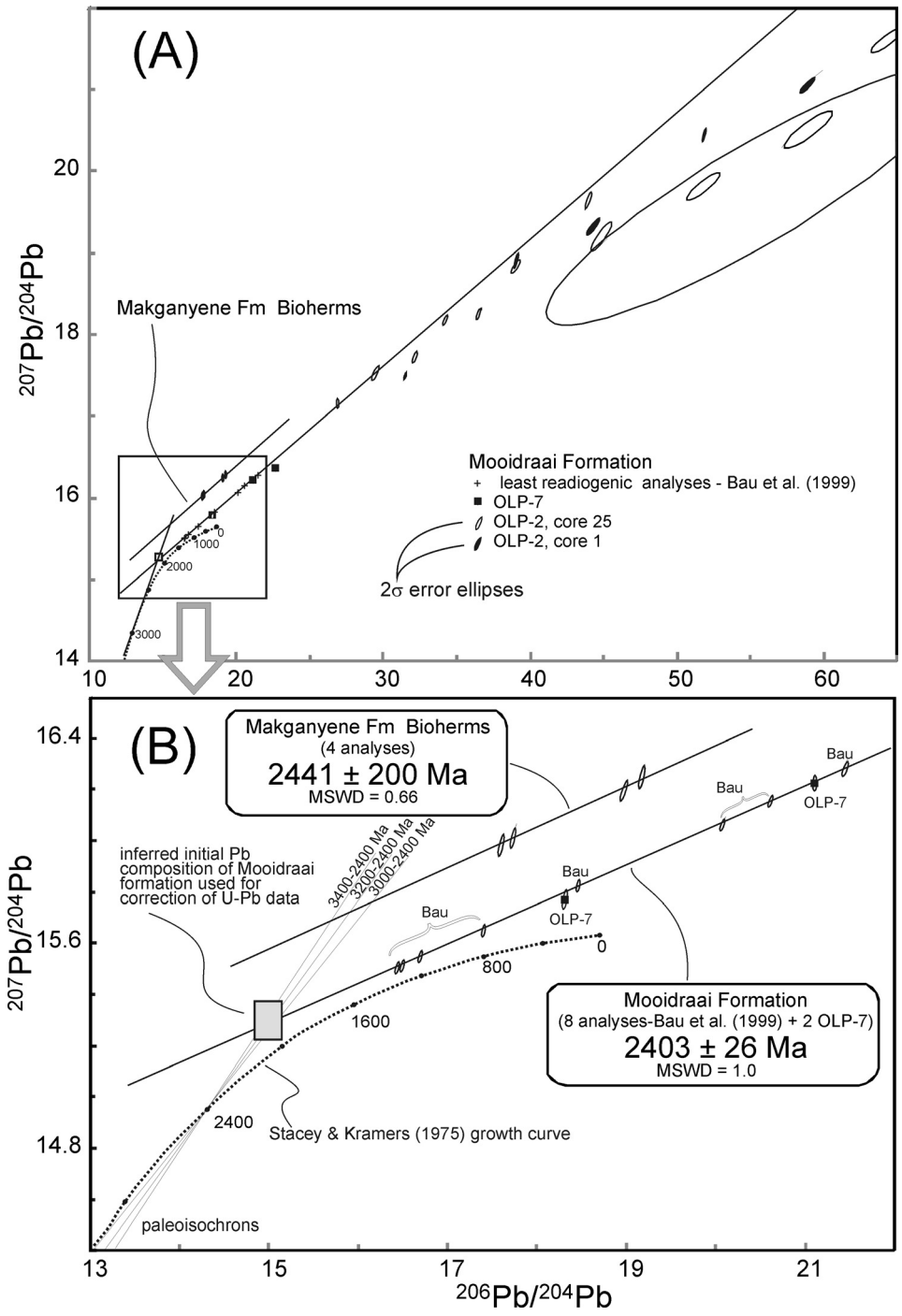

Fig. 7. (A and B) Pb–Pb diagram for data of Mooidraai Formation and Makganyene Formation carbonates, plotted together with a selection of data from Bau et al. (1999). See text for discussion.

in the literature. Previous studies have observed riebeckite as a minor to trace component of the Hotazel Formation (Tsikos and Moore, 1997). Fibrous riebeckite ("crocidolite") from the stratigraphically older Kuruman BIF of the Ghaap Group appears to have a structurally controlled distribution (Dreyer and Söhnge, 1992). By contrast, the samples described in this paper show no evidence of a cross-cutting relationship between the riebeckite-rich assemblages and the microbands of the host BIF (Fig. 4B–D). We thus tentatively interpret the development of riebeckite in our rocks as indicative of the diagenetic – and possibly primary depositional – environment of the Hotazel–Mooidraai transition, whereby the facies change between BIF and carbonate sedimentation would have been accompanied by an attendant increase in salinity of the ambient water column and pore waters in the initial sediments.

6.2. Age of formation of stylolites in the Mooidraai Formation

The strong variation in the degree of discordance of the U–Pb analyses of the Mooidraai samples is a function of the U content, as shown by the correlation between U content and $^{206}Pb/^{238}U$ age of the analyses (inset in Fig. 8). The U content correlates, in turn, with the presence and abundance of black coatings, which correspond to the stylolites.

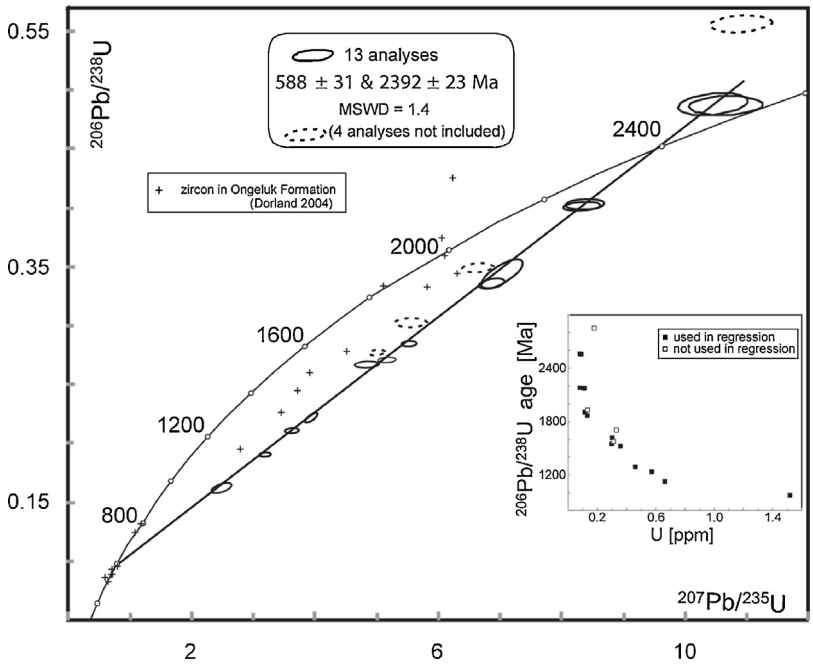

Fig. 8. Concordia diagram with U–Pb data of Mooidraai Formation. Insert demonstrates the relationship between U content and $^{206}Pb/^{238}U$ ages. Also shown are SIMS results on zircon from the Ongeluk Formation by Dorland (2004). Error ellipses represent 2σ.

These features provide three possible explanations for the U–Pb discordance. The first interpretation is that the stylolites developed already during early diagenesis and burial and during this process captured U. The extensive formation of riebeckite in concordant seams and layers can be explained as a response to the addition of Na from early basinal brines. Uranium is soluble in oxidizing fluid and it can be transported by basinal brines (*e.g.* Lehmann, 2008). The U present in the original carbonate deposits may also have been purged and concentrated into the stylolites, along with the other impurities, during the dissolution–reprecipitation processes. Later disturbances in the Neoproterozoic, most likely fluid related events, would have affected these stylolite layers causing Pb loss and creating the discordia array.

The second interpretation is that U was introduced by fluids from external sources into the system in the late Neoproterozoic and was stored in pre-existing stylolites. Such fluids would have had oxidizing qualities, capable of transporting U, which would then be trapped by reduction barriers at the stylolite interfaces. Some evidence for the reality of such secondary fluids in the Transvaal basin are discussed below. This interpretation implies that the discordia line is a mixing line between the time of formation of the carbonates at ~2400 Ma and that of U-enrichment at 588 Ma.

The third possibility is an expansion of the second, implying not only that U was introduced in the late Neoproterozoic, but that stylolites themselves were produced during this event reflecting the action of regional stresses and fluids. A consideration supporting this view is that diagenetic compaction would likely have affected the entire basin in somewhat uniform ways and it is thus not evident why carbonates with broadly similar levels of impurities would not have developed equal densities of diagenetic stylolites everywhere. The considerable variations in the development of

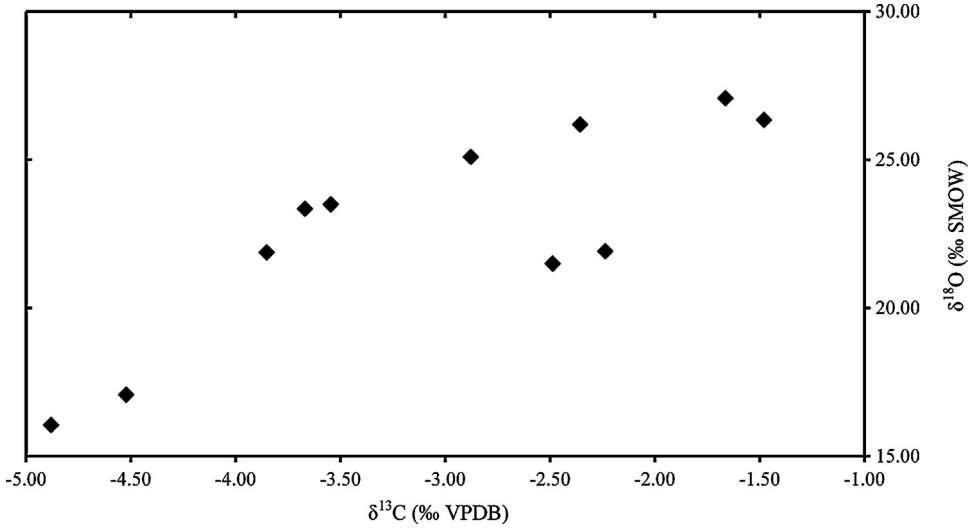

Fig. 9. Plot of $\delta^{13}C$–$\delta^{18}O$ for Makganyene Formation bioherm carbonates.

stylolites, and the associated U–Pb behavior, across the region are easier to envisage assuming a superimposed stress regime, which localized deformation and fluid flow along preferred zones.

One important argument in favor of the secondary, Neoproterozoic introduction of U, whether related to the formation of stylolites or not, is the correlation between U–Pb discordance and U content. If fluids had just leached existing Pb from these rocks at 588 Ma, it is not evident why they would have acted solely along these thin secondary layers, leaving the Pb in the intervening carbonate much less affected by the process, especially when considering that the Pb concentration in different parts of the rock are fairly similar (Table 2). A further argument along the same lines is that there is very little evidence for disturbed Pb–Pb systematics in the carbonates that lack stylolites, such as in the three samples from core OLP-7 (Tsikos et al., 2001), the Mooidraai samples studied by Bau et al. (1999) as well as the Makganyene bioherm samples.

The possible effect of superimposed fluid alteration on the Mooidraai Formation must be assessed in light of similar processes that have been recorded in the broader geographical region of, and at various stratigraphic levels across, the Transvaal Supergroup. Several events of large scale fluid migration and hydrothermal processes influencing mineralogy and ore concentration in this region have been proposed. Duane et al. (2004) have argued for a craton-wide epigenetic fluid-infiltration event as the responsible process for deposition of Pb–Zn deposits in the Campbellrand Subroup carbonates of the Transvaal Supergroup. In the northernmost part of the Kalahari Manganese Field, the Hotazel manganese ores and adjacent BIF have undergone metasomatic alteration with key geochemical characteristic being the introduction of alkalis (mainly Na and K) to the rocks by hydrothermal fluids (Gnos et al., 2003; Tsikos and Moore, 2005). Attempts to date this alteration process have utilized primarily the Ar–Ar dating technique on related potassic alteration minerals: sugilite (an alkali-rich Mn-silicate) from the Wessels mine yielded an age of 1048 ± 6 Ma while the co-existing Mn-mica norrishite appeared to be slightly younger at ~800 Ma (Gnos et al., 2003). Similar alkali-rich assemblages were investigated by Moore et al. (2011) from the manganiferous footwall of hematite iron-ores at Bruce Mine, some 80 km south of the northernmost Kalahari Manganese Field. In spite of the close mineralogical similarities between the alkali-rich metasomatic assemblages at the above two localities, and the stratigraphic proximity of both assemblages to the regional Transvaal–Olifantshoek unconformity as a plausible fluid-flow pathway, the single-grain Ar–Ar dating of hydrothermal sugilite from the Bruce material gave an age of 620 ± 3 Ma.

The 620 Ma sugilite Ar–Ar age is arguably the one that compares the closest to the ~588 Ma age of the Mooidraai stylolites reported herein. Assigning these two ages to a single, regional-scale fluid-flow event may appear ambitious at this stage, given the geographic distance and mineralogical and stratigraphic contrasts between the two localities in question. However, further evidence for overprinting fluid events in the region can also be sought in the zircon data reported by Dorland (2004) from the Ongeluk lavas, which comprise a significant component of Neoproterozoic analyses besides highly discordant older ones. The data of Dorland (2004), shown for comparison in Fig. 8, plot to the left of the Mooidraai discordia line, and provide evidence for various disturbances in the late Paleoproterozoic and the Neoproterozoic. These events may also be responsible for the deviation from the discordia line of four analyses as we observe in drillcore OLP-2 (Fig. 8).

6.3. Primary age of the Mooidraai Formation and Makganyene Formation bioherms

The U–Pb age of 2392 ± 23 Ma obtained in this study for the Mooidraai Formation corresponds within error to that determined by Pb–Pb alone by Bau et al. (1999) on its dolomitized and silicified counterpart. In conjunction with the 2441 ± 200 Ma age reported in this paper for the Makganyene Formation bioherms, we regard the above age agreement as particularly significant for the following reasons:

(1) It lends support to recent results of detrital zircon dating studies from the upper Makganyene and lower Hotazel Formations, which did not discover any zircons younger than 2436 Ma (Moore et al., 2012);
(2) It strengthens the argument that the Pb–Pb whole rock age of 2222 ± 12 Ma reported by Cornell et al. (1996) for the Ongeluk andesites is too young. These authors document a very extensive alteration of the volcanic rocks, attributing these effects mainly to sea water processes. The Pb–Pb data that define the age are collinear, but the age is controlled strongly by the very radiogenic composition of a pillow rim. The U gain of this rim is interpreted by these authors to result from seawater alteration, but it could equally well have been the results of much later events causing a rotation of the isochron. A superimposed late Mesoproterozoic alteration event is indeed recorded in these rocks by the Rb–Sr system (Cornell et al., 1996).
(3) It reinforces the notion that, irrespective of whether or not there is an unconformable relationship between the Ghaap and Postmasburg Groups in the Transvaal Supergroup as argued elsewhere, no hiatus of *ca.* 200 m.y. needs to be invoked between the above two groups (Moore et al., 2001, 2011; Polteau et al., 2006).

Arguably, the most important implication of the foregoing points concerns global palaeo-environmental models as proposed for the early Palaeoproterozoic, with specific regard to the chronostratigraphic placement of the Mooidraai and Hotazel formations in relation to the timing of the Great Oxidation Event (GOE) at *ca.* 2340 Ma (Bekker et al., 2004). A pre-2400 Ma age for the Hotazel manganese ores and host BIF places the formation of these deposits at a time immediately prior to the GOE, and renders them as a potentially very important proxy for the environmental and biological changes that accompanied the atmosphere-ocean system over the transition from an oxygen-free to and oxygen-rich world (Tsikos et al., 2010).

7. Concluding remarks

The U–Pb system demonstrates that the carbonates of the Mooidraai Formation sampled in drillhole OLP-2 have been strongly affected by metasomatic processes, likely connected to compression that developed stylolites by dissolution–reprecipitation processes. There is strong evidence that U was introduced U in the system at 588 ± 31 Ma, although it is still uncertain whether the stylolites developed at the same time or whether they were pre-existing features that just trapped incoming U. The resulting variation in U–Pb discordance defines a discordia line with an upper intercept age of 2392 ± 23 Ma, which confirms the Pb–Pb age of 2394 ± 23 Ma previously established for dolomitized Mooidraai carbonate at a different location (Bau et al., 1999). Evidently the dolomitization process had affected the chemical composition of the carbonate, removing, for example, most of the Sr present in undolomitized carbonate, a feature previously also observed by Frauenstein et al. (2009). The dolomitized carbonates remained subsequently screened from the later metasomatic and deformational event, which is recorded instead in our samples where it resulted in fully disturbed Pb–Pb systematics (Fig. 7A). This diverse behavior of carbonates reflects previous experience in dating carbonates of different ages. In a number of experiments, the Pb–Pb and

U–Pb studies yielded results interpreted to date, or be close to, the age of deposition and/or diagenesis (Moorbath et al., 1987; Smith and Farquhar, 1989; Jahn et al., 1990; Walker et al., 2006). By contrast, Jahn (1988) documented widespread resetting by recrystallization of marbles during metamorphism. Similar cases of complex U–Pb behavior were discussed by Jahn and Cuvellier (1994).

The strong discrepancy in the Pb initial ratio between the isochrons for the Mooidraai and Makganyene carbonates points to another possible approach to evaluating primary from secondary origins of isochrons. The Makganyene line (Fig. 7B) projects toward a much higher $^{207}Pb/^{204}Pb$ initial ratio than for the Mooidraai carbonates, indicating the much more dominant control by old crustal sources in the former. By contrast, the less radiogenic Mooidraai initial Pb composition ($^{206}Pb/^{204}Pb = 15.0$, $^{207}Pb/^{204}Pb = 15.3$) can be compared with the equally less radiogenic Sr-isotope signature ($^{87}Sr/^{86}Sr = 0.7031$) of the approximately contemporaneous (Moore et al., 2001) Duitschland Formation (Frauenstein et al., 2009). The isotopic and chronostratigraphic similarities and the potentially comparable palaeoenvironmental significance of the Mooidraai and Duitchland Formations in the context of early Earth evolution, should therefore constitute a future research focus in the region.

Acknowledgments

Access to drillcores OLP-2 and -7 for the purposes of this study was kindly provided by the geology office of BHP-Billiton in Hotazel, South Africa, and specifically by Mr. E.P. Ferreira and Mr. T. Rambuda, to whom we extend our sincerest appreciation and thanks. We also wish to thank Dr. B. Kuhn, Prof. J.S. Marsh (Rhodes University) and Prof. C. Harris (University of Cape Town), for their assistance with the microprobe/SEM-EDS, XRF and stable isotope analyses respectively. Constructive comments by M. Bau and two anonymous reviewers are gratefully acknowledged.

References

Bau, M., Romer, R.L., Luders, V., Beukes, N.J., 1999. Pb, O, and C isotopes in silicified Mooidraai dolomite (Transvaal Supergroup, South Africa): implications for the composition of Palaeoproterozoic seawater and dating the increase of oxygen in the Precambrian atmosphere. Earth and Planetary Sciences Letters 174, 43–57.

Bau, M., Alexander, B., 2006. Preservation of primary REE patterns without Ce anomaly during dolomitization of Mid-Paleoproterozoic limestone and the potential re-establishment of marine anoxia immediately after the Great Oxidation Event. South African Journal of Geology 109, 81–86.

Bekker, A., Holland, H.D., Wang, P.-L., Rumble III, D., Stein, H.J., Hannah, J.L., Coetzee, L.L., Beukes, N.J., 2004. Dating the rise of atmospheric oxygen. Nature 427, 117–120.

Beukes, N.J., 1983. Palaeoenvironmental setting of iron-formations in the depositional basin of the Transvaal Supergroup, South Africa. In: Trendall, A.F., Morris, R.C. (Eds.), Iron-formation: Facts and Problems, vol. 1. Elsevier, Amsterdam, pp. 131–209.

Beukes, N.J., Gutzmer, J., Mukhopadhyay, J., 2003. The geology and genesis of high-grade hematite iron ore deposits. Transactions of the Institution of Mining and Metallurgy 112, B18–B25.

Corfu, F., 2004. U–Pb age, setting and tectonic significance of the anorthosite–mangerite–charnockite–granite suite, Lofoten-Vesterålen, Norway. Journal of Petrology 45, 1799–1819.

Cornell, D.H., Schutte, S.S., Eglington, B.L., 1996. The Ongeluk basaltic andesite formation in Griqualand West, South Africa: submarine alteration in a 2222 Ma Proterozoic sea. Precambrian Research 79, 101–124.

Craddock, P.R., Dauphas, N., 2011. Iron and carbon isotope evidence for microbial iron respiration throughout the Archean. Earth and Planetary Science Letters 303, 121–132.

Dorland, H.C., 2004. Provenance ages and timing of sedimentation of selected Neoarchean and Paleoproterozoic successions on the Kaapvaal craton. PhD thesis (unpublished), Rand Afrikaans University, 326 pp.

Dreyer, C.J.B., Söhnge, A.P.G., 1992. The crocidolite and amosite deposits of the Republics of South Africa and Bophuthatswana. Handbook, Geological Survey of South Africa 12, 126.

Duane, M.J., Kruger, F.J., Turner, A.M., Whitelaw, H.T., Coetzee, H., Verhagen, B., 2004. The timing and isotopic character of regional hydrothermal alteration and associated epigenetic mineralisation in the western sector of the Kaapvaal craton (South Africa). Journal of African Earth Sciences 38, 461–476.

Frauenstein, F., Veizer, J., Beukes, N., van Niekerk, H.S., Coetzee, L.L., 2009. Transvaal Supergroup carbonates: implications for Paleoproterozoic $\delta^{18}O$ and $\delta^{13}C$ records. Precambrian Research 175, 149–160.

Gnos, E., Armbruster, T., Villa, I.M., 2003. Norrishite, $K(Mn_2^{3+}Li)Si_4O_{10}(O)_2$, an oxymica associated with sugilite from the Wessels Mine, South Africa: crystal chemistry and $^{40}Ar–^{39}Ar$ dating. American Mineralogist 88, 189–194.

Guo, Q., Strauss, H., Kaufman, A.J., Schröder, S., Gutzmer, J., Wing, B., Baker, M.A., Bekker, A., Jin, Q., Kim, S-T., Farquhar, J., 2009. Reconstructing Earth's surface oxidation across the Archean–Proterozoic transition. Geology 37, 399–402.

Hannah, J.L., Bekker, A., Stein, H.J., Markey, R.J., Holland, H., 2004. Primitive Os and 2316 Ma age for marine shale: implications for Paleoproterozoic glacial events and the rise of atmospheric oxygen. Earth Planetary Sciences Letters 225, 43–52.

Heimann, A., Johnson, C.M., Beard, B.L., Valley, J.W., Roden, E.E., Spicuzza, M.J., Beukes, N.J., 2010. Fe, C, and O isotope compositions of banded iron formation carbonates demonstrate a major role for dissimilatory iron reduction in 2.5 Ga marine environments. Earth and Planetary Sciences Letters 294, 8–18.

Holland, H.D., Beukes, N.J., 1990. A paleoweathering profile from Griqualand West, south Africa: evidence for a dramatic rise in atmospheric oxygen between 2.2 and 1.9 bybp. American Journal of Science 290-A, 1–34.

Jaffey, A.H., Flynn, K.F., Glendenin, L.E., Bentley, W.C., Essling, A.M., 1971. Precision measurement of half-lives and specific activities of ^{235}U and ^{238}U. Physical Review, Section C, Nuclear Physics 4, 1889–1906.

Jahn, B.M., 1988. Pb–Pb dating of young marbles from Taiwan. Nature 332, 429–432.

Jahn, B.M., Bertrand-Sarfati, J., Morin, N., Macé, J., 1990. Direct dating of stromatolitic carbonates from the Schmidtsdrif Formation (Transvaal Dolomite), South Africa, with implications on the age of the Ventersdorp Supergroup. Geology 18, 1211–1214.

Jahn, B.M., Cuvellier, H., 1994. Pb–Pb and U–Pb geochronology of carbonate rocks: an assessment. Chemical Geology 115, 125–151.

Johnson, C.M., Beard, B.L., Klein, C., Beukes, N.J., Roden, E.E., 2008. Iron isotopes constrain biologic and abiologic processes in banded iron formation genesis. Geochimica et Cosmochimica Acta 72, 151–169.

Lehmann, B., 2008. Uranium ore deposits. Reviews in Economic Geology 2, 16–26.

Ludwig, K.R., 2003. Isoplot 3.0. A Geochronological Toolkit for Microsoft Excel: Berkeley Geochronology Center Special Publication No. 4, 70 pp.

Melezhik, V.A., 2006. Multiple causes of Earth's earliest global glaciation. Terra Nova 18, 130–137.

Merino, E., Canals, A., 2011. Self-accelerating dolomite-for-calcite replacement: self-organized dynamics of burial dolomitization and associated mineralization. American Journal of Science 311, 573–607, http://dx.doi.org/10.2475/07.2011.01.

Moorbath, S., Taylor, P.N., Orpen, J.L., Treloar, P., Wilson, J.F., 1987. First direct radiometric dating of Archaean stromatolitic limestone. Nature 326, 865–867.

Moore, J.M., Tsikos, H., Polteau, S., 2001. Deconstructing the Transvaal Supergroup, South Africa: implications for Paleoproterozoic paleoclimate models. Journal of African Earth Sciences 33, 437–444.

Moore, J.M., Polteau, S., Armstrong, R.A., Corfu, F., Tsikos, H., 2012. The age and correlation of the Postmasburg Group, southern Africa: Constraints from detrital zircon grains. Journal of African Earth Sciences 64, 9–19.

Moore, J.M., Kuhn, B.K., Mark, D.F., Tsikos, H., 2011. A sugilite-bearing assemblage from the Wolhaarkop breccia, Bruce iron-ore mine, South Africa: evidence for alkali metasomatism and $^{40}Ar–^{39}Ar$ dating. European Journal of Mineralogy 23, 661–673.

Norrish, K., Hutton, J.T., 1969. An accurate X-ray spectrographic method for the analysis of a wide range of geological samples. Geochimica et Cosmochimica Acta 33, 431–453.

Polteau, S., Moore, J.M., Tsikos, H., 2006. The geology and geochemistry of the Palaeoproterozoic Makganyene diamictite. Precambrian Research 148, 257–274.

Smith, P.E., Farquhar, R.M., 1989. Direct dating of Phanerozoic sediments by the $^{238}U–^{206}Pb$ method. Nature 341, 518–521.

Stacey, J.S., Kramers, J.D., 1975. Approximation of terrestrial lead isotope evolution by a two-stage model. Earth and Planetary Sciences Letters 26, 207–222.

Tsikos, H., Moore, J.M., 1997. Petrography and geochemistry of the Paleoproterozoic Hotazel iron-formation, Kalahari Manganese Field, South Africa: implications for Precambrian manganese metallogenesis. Economic Geology 92, 87–97.

Tsikos, H., Moore, J.M., Harris, C., 2001. Geochemistry of the Palaeoproterozoic Mooidraai Formation: Fe-rich limestone as end-member of iron formation deposition, Kalahari Manganese Field, Transvaal Supergroup, South Africa. Journal of African Earth Sciences 32, 19–27.

Tsikos, H., Beukes, N.J., Moore, J.M., Harris, C., 2003. Deposition, diagenesis, and secondary enrichment of metals in the Paleoproterozoic Hotazel iron formation, Kalahari Manganese Field, South Africa. Economic Geology 98, 1449–1462.

Tsikos, H., Moore, J.M., 2005. Sodic metasomatism in the Palaeoproterozoic Hotazel iron-formation, Transvaal Supergroup, South Africa: implications for fluid-rock interaction in the Kalahari manganese field. Geofluids 5, 264–271.

Tsikos, H., Matthews, A., Erel, Y., Moore, J.M., 2010. Iron isotopes constrain biogeochemical redox cycling of iron and manganese in a Paleoproterozoic stratified basin. Earth and Planetary Sciences Letters 298, 125–134.

Walker, J., Cliff, R.A., Latham, A.G., 2006. U–Pb Isotopic Age of the StW 573 Hominid from Sterkfontein, South Africa. Science 314, 1592–1594.

Walraven, F., Armstrong, R.A., Kruger, F.J., 1990. A chronostratigraphic framework for the north-central Kaapvaal Craton, the Bushveld Complex and Vredefort Structure. Tectonophysics 171, 23–48.